

Development of Battery-Less Wireless Current Sensor Node Utilizing Charging Time of Capacitors with Wide Measurement Range

Hironao Okada, Toshihiro Itoh

National Institute of Advanced Industrial Science and Technology, Tsukuba, Japan
Email: hironao.okada@aist.go.jp

Received October 24, 2013; revised November 12, 2013; accepted November 18, 2013

Copyright © 2013 Hironao Okada, Toshihiro Itoh. This is an open access article distributed under the Creative Commons Attribution License, which permits unrestricted use, distribution, and reproduction in any medium, provided the original work is properly cited.

ABSTRACT

We report a novel battery-less wireless current sensor node without an analog to digital converter (ADC). If a capacitor is charged using a current transformer (CT) and a rectifying circuit, the charging time depends on the current flowing through a power line. In the case that the node transmits data every time when voltage of the capacitor exceeds a threshold voltage, we can indirectly measure the current by measuring the transmission intervals. In this method, the circuit of the node can be simplified and power consumption for the wireless transmission can be decreased because the measured current data does not need to be included in the transmitted packet. However, the measurable range is about single digit because the transmission interval decreases suddenly as the current increases. In this work, we have expanded the range using one CT, one wireless transmission module, and two charging circuits that include different load resistors connected in series. The results indicated that the measurable range was from 0.5 A to 50 A.

Keywords: Battery-Less; Wireless Current Sensor Node; Power Monitoring

1. Introduction

Wireless sensor networks are expected to be utilized for health [1] and security applications [2] as well as environmental monitoring [3] and could enable real-time visualization and control of power consumption so that energy efficiency is improved. This is very attractive for the energy management systems in a lot of facilities, such as offices, factories and homes. A wireless current sensor with a current transformer (CT) is useful tool especially to install in existing facilities because the wiring work is not needed [4]. However, the nodes must be made battery-less type to be widely used [5].

Our research team has been developing a battery-less wireless current sensor node for an electrical power monitoring system [5]. A current value is generally measured by an analog to digital conversion (ADC) of the voltage at a load resistor connected to a CT. This type of node can measure current with high accuracy using an ADC and an amplifier, and transmit data at a constant time interval. However, since this node needs power for an ADC and a timer to operate intermittently, a rechargeable battery and charging circuit with an over-

charged protection are required.

Our battery-less wireless current sensor node is composed of simple circuits without an ADC and a rechargeable battery. This node transmits data using the power charged in a chip capacitor with a CT from a power line every time when the power is charged enough for wireless transmission. In this system, the time intervals between the transmissions are depend on the current flowing through a power line. Therefore the current value can be deduced by measuring the transmission intervals. In this node, because an ADC is not needed, a simple circuit can be realized. In addition, since measured current data does not need to be included in the transmitted packet, the power consumption for the wireless transmission can be decreased. However, the node has a demerit that the measurable range is about single digit because the transmission interval decreases suddenly as the current increases. In this paper, we report a method for expanding the current measurable range up to double digits.

2. Design

The developed node transmits data using power charged

in a capacitor every time when a voltage of the capacitor exceeds a threshold voltage V_{th} . The charged power is consumed, then the voltage of the capacitor drops to the minimum voltage V_{min} . **Figure 1(a)** shows the basic model of this circuit. Since the current obtained from a CT is rectified, the module composed of the CT and the rectifying circuit represent DC power source as the equivalent circuit in this figure. The power control circuit detects enough power charged in the capacitor C and provides the power to the wireless transmission module by the switch. Time interval t between the transmissions is expressed by following equation derived from the equation of capacitor charging.

$$t = -CR_{lim} \log \left[\frac{E - V_{th}}{E - V_{min}} \right] \quad (1)$$

where C is the capacitor to charge the power, R_{lim} is a current limiting resistor, and E is a rectified and smoothed voltage generated from a CT. E is expressed as:

$$E = KI_0R_L/n \quad (2)$$

where K is coupling coefficient of a CT, I_0 is current flowing through a power line, R_L is a load resistor, and n is a turn ratio of a CT. **Figure 1(b)** shows transmission intervals at the case that C is 100 μF , R_{lim} is 1 $\text{k}\Omega$, V_{th} is 2.1 V, and V_{min} is 1.8 V. Since the time interval t drops rapidly as E increases, the resolution at high current becomes low. The maximum measurable range mainly depends on variability of the time interval caused by ripples generated from a rectification circuit and noises. On the other hand, the minimum measurable range depends on the power consumption of the power control circuit and on the power obtained from the CT. The measurable range does not expand dramatically even if the minimum and maximum limit can be improved.

Although the easiest method to increase the measurable range is to use multiple nodes with different load resistors, the cost of the manufacturing and installation increases. In this research, we have developed a method to expand the range using one CT, one wireless transmis-

sion module, and two charging circuits that include different load resistors connected in series.

The challenge is how this type of node detects measuring current I_0 by itself to switch two charging circuits. If E can be measured, I_0 can be calculated using Equation (1). In this node, however, E cannot be measured if E is higher than V_{th} . Because if the voltage of C exceeds V_{th} , the power charged in C is consumed for wireless transmission. In this development, we have proposed a method to detect increasing rate of voltage of C .

Figure 2 shows a proposed circuit without bypass capacitors, current-limiting resistors, damping resistors, and voltage reference generators. The resistors R_0 and R_{11} are load resistors for the CT. The circuit A including R_0 and B including R_{11} are for measuring low and high current flow, respectively. The devices $U_{0-4,10,11}$ are comparators and $U_{5-9,12}$ are analog switches. The Cockcroft-Walton (CW) circuits [6] are used as stepup converter in both circuit A and B. The power sources of the devices U_{0-9} and the others U_{10-12} are charged capacitor C_0 and C_4 , respectively. The all voltage references V_{ref} are same value and generated by bandgap reference generators in both circuits. The circuit A has the circuit A1 and A2 to change the power source for the wireless transmission module depending on current flowing through a power line. The circuit A1 switches the charging circuit from the circuit A to B if the measuring current exceeds a threshold value. The circuit A2 turns the charging circuit back.

Figure 3 shows the relationship between measuring current I_0 and the charging circuits. I_A and I_B represent I_0 when power charged by the circuit A and B is used for wireless transmission, respectively. I_{th_up} and I_{th_down} are threshold current for switching the charging circuit from the circuit A to B and from the circuit B to A, respectively. These threshold values are set different values to make behaviors of this circuit stable.

Figure 4 shows the voltage changes at the points V_{0-6} of the circuit in **Figure 2**. **Figures 4(a)** and **(b)** indicate the case of low and high current I_0 , respectively. V_{T1} , V_{T2} , V_{T3} , and V_{T4} represent the threshold voltages for V_0 at U_0 , U_1 , U_2 , and U_{10} , respectively. V_Z shows the zener voltage of DZ_0 and DZ_1 .

First, behaviors of the circuit in the case of **Figure 4(a)** are explained below. When current I_A flows through a measured power line, voltage V_0 exceeds V_{T1} , but V_5 does not increase up to V_{T1} . When V_0 increases up to V_{T1} , the output of comparator U_0 changes from low to high level. The resistor R_7 and the capacitor C_2 compose a delay circuit. The voltage V_2 increases up to the voltage produced by a voltage divider (R_7 and R_9) according to the time constant ($R_7 \times C_2$). When V_2 increases up to V_{ref} , the output of the comparator U_3 becomes high level. Using this delay circuit and the comparator U_1 , whether the increasing

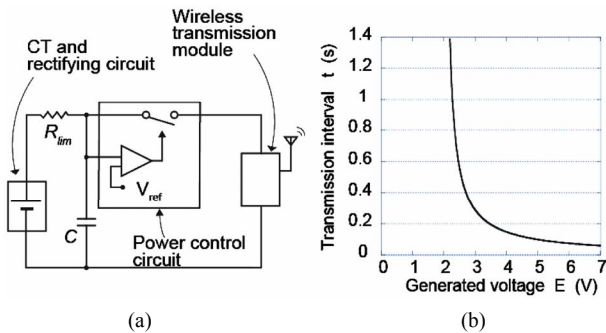


Figure 1. (a) Basic model of the circuit for the developed node. (b) Transmission interval at the case that C is 100 μF , R_{lim} is 1 $\text{k}\Omega$, V_{th} is 2.1 V and V_{min} is 1.8 V.

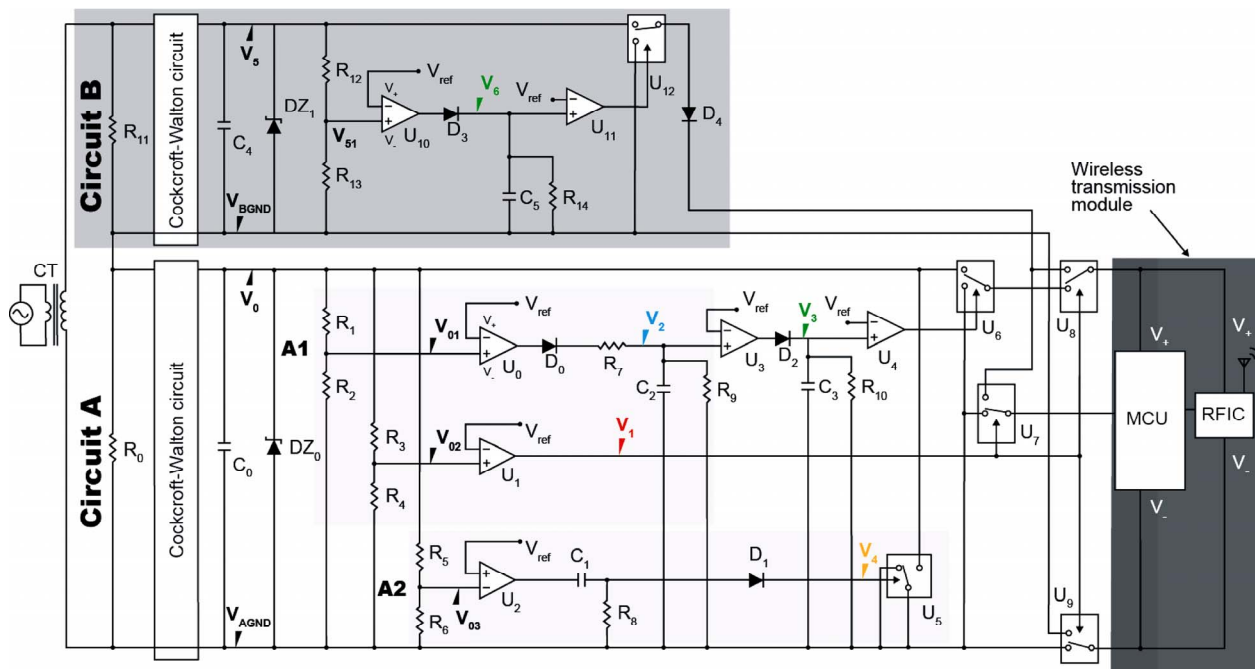


Figure 2. Schematic circuit diagram for battery-less wireless current sensor node using two different load resistor.

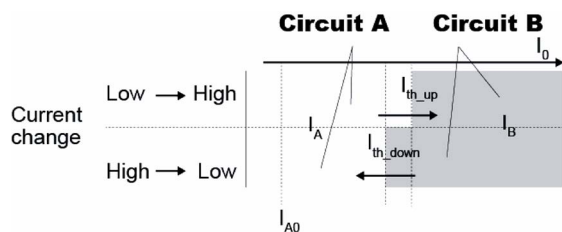


Figure 3. Relationship between measuring current I_0 and charging circuits.

rate of V_0 exceeds a threshold voltage can be detected. In other words, if V_0 increases up to V_2 during the delay, this circuit can detect that I_0 exceeds I_{th_up} . In the case of **Figure 4(a)**, I_0 is less than I_{th_up} . When the output of the comparator U_3 becomes high level, the output of the comparator U_4 also changes to high level immediately. The analog switch U_6 connects C_0 to the wireless transmission module, then the module starts wireless transmission. At this time, V_0 drops without delay, then output of U_0 becomes low level. However, the output of U_4 keeps high level by the delay circuits composed of C_2 , R_9 , C_3 , and R_{10} until the wireless transmission finishes. U_8 and U_9 are analog switches for switching the power sources charged by the circuit A or B. The output of analog switch U_7 indicates which power source is used. Low and high level of output of U_7 shows that the wireless transmission is performed using the power charged by the circuit A and B, respectively. The transmitted packet includes an identification number of the wireless sensor node and one bit data that indicates which power source is used, but does not include current data.

In **Figure 4(b)**, V_0 exceeds V_{T2} during the above mentioned delay, then the output of comparator U_1 becomes high level. The analog switches U_8 and U_9 change the power source from C_0 to C_4 and the output of analog switch U_7 changes the connection of a micro controller unit (MCU) from V_{AGND} to the analog switch U_{12} . At this time, since the power charged in C_0 is not used for the wireless transmission, V_0 increases up to the voltage which depends on the power consumption of circuit A and the power obtained from the CT. In this case, although V_0 can exceed withstand voltages of the devices used in the circuit A, the zener diode DZ_0 is used to prevent breakdowns of the devices. In the circuit B, wireless transmission is performed like the circuit A every time when the voltage V_5 increases up to V_{T4} . At the connection between U_{12} and the circuit A, influence of pulsating voltage must be prevented. Although V_5 is DC voltage if V_{BGND} is the reference voltage, V_5 is pulsating voltage if V_{AGND} is the reference voltage. Since behavior of U_{12} can be unstable by the pulsating voltage, the effect is decreased using the diode D_5 .

When I_0 decreases from I_B to I_{th_down} , V_0 does not decrease to V_{T2} . Because the power consumption of the circuit A except for wireless transmission is small. Actually, V_0 does not decrease to V_{T2} unless I_0 decreases to around minimum of the measurable range. The current I_{A0} in **Figure 3** indicates I_0 at which V_0 decreases to V_{T2} . In this case, the power charged by the circuit B cannot be charged enough for the wireless transmission if I_0 is lower than I_{th_down} . Thus, the power charged by the circuit A must be used for the wireless transmission at less than

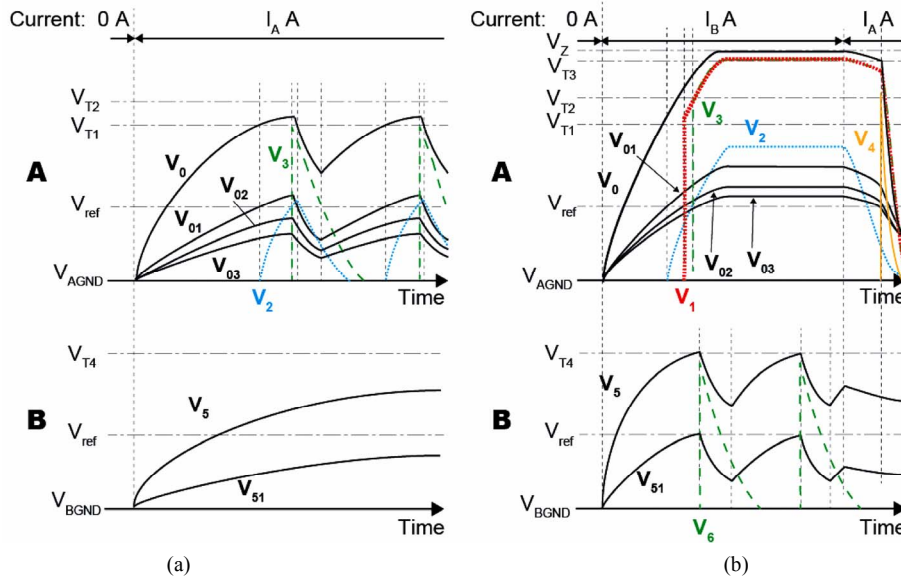


Figure 4. Voltage changes at the points V_{0-6} of the circuit in Figure 2. (a) and (b) indicate the case of low and high current I_0 , respectively.

I_{th_down} . To change the power source, V_0 need to be decreased to less than V_{T2} . The circuit A2 can detect an event at which I_0 decreases to I_{th_down} and decrease V_0 . The output of the comparator U_2 becomes high level when V_0 decreases to the voltage V_{T3} at which I_0 is I_{th_down} . This high level signal must be changed to low level immediately after V_0 decrease to V_{T2} . Because U_5 continues to connect V_0 and V_{AGND} if the output of U_2 is high level. In this case, power cannot be charged in C_0 . To make one shot pulse signal, this high level signal is differentiated by a differentiator composed of the capacitor C_1 and the resistor R_8 . The analog switch U_5 connects V_{AGND} with V_0 through a current limiting resistor only for the time of the pulse width, then V_0 drops to less than V_{T2} . The diode D_3 is intended for preventing a signal which is generated when the output of U_2 changes from high to low level. If D_3 is not in this circuit, the circuit B cannot be used to charge the power for wireless transmission. Because the power is consumed every time when V_0 exceeds V_{T3} .

3. Experimental Result

In this research, we designed wireless current sensor node with measurable range from 0.5 A to 50 A in which the transmission intervals are less than 0.5 s. The 3 stage CW circuit was used in the circuit A and B. We have not examined how many stages of the CW and how much capacitors used in the CW circuit are suitable for this current sensor.

Table 1 shows the designed values of the resistors and the capacitors. The resistance values of $R_{1-6,12,13}$ which always consume the current were more than 10 M Ω to reduce the power consumption. CTL-10-CLS (UR_D),

MCP644x (MICROCHIP), ADG849 (ANALOG DEVICES) and LTC1540 (LINER TECHNOLOGY) were used as a CT, comparators, analog switches, voltage reference generators, respectively. A wireless sensor module was mainly composed of C8051F930 (Silicon labs) used as MCU and nRF24L01 (Nordic) used as RF IC. The voltage reference was 1.182 V [7]. The conditions [5] of the wireless transmission were same with except for the packet structure. Since the lower limit voltage at which both two ICs work was 1.8 V [8,9], V_{T1} must be more than 1.8 V. In this research, we determined V_{T1} was 2.15 V. In this case, since the required charge for the wireless transmission was about 4.18 μ As [5], the capacitance values of C_0 and C_4 must be more than 11.9 μ F. On the other hand, these capacitors have a function to smooth ripples. In this research, we determined the capacitance values of C_0 and C_4 were 0.8 mF and 1.3 mF, respectively. The reason that the capacitance of C_4 is larger than C_0 is that I_B is higher than I_A . The resistance values of $R_{10,14}$ and the capacitance values $C_{3,5}$ were determined according to [5]. The output voltage of the CW circuit depends on the load. First, the resistance values of R_{1-6} were temporarily set to 10 M Ω in order to fix the load. Next, resistance value of R_0 by which V_0 exceeds the V_{T1} when I_0 is 0.5 A was determined. Not to become the transmission interval (t_{trans}) short, small resistance is better. In this research, we determined the resistance value of R_0 was 6.2 k Ω . In this case, the transmission intervals were almost not changed if I_0 exceeded about 6 A. Thus, we determined I_{th_up} and I_{th_down} were 6.5 A and 6 A, respectively. The resistance values of $R_{3,4,7,9}$ and capacitance value of C_2 were set to change the output of U_1 to high level at the I_{th_up} . In this case, V_{T2} was 2.29 V.

Table 1. Values of the resistors and capacitors in Figure 2.

Resistor	Resistance (Ω)	Capacitor	Capacitance (F)
R_0	6.2 k	C_0	1.3 m
R_1	10 M	C_1	1 μ
R_2	12.2 M	C_2	0.2 μ
R_3	10 M	C_3	0.02 μ
R_4	10.68 M	C_4	0.8 m
R_5	20.51 M	C_5	0.02 μ
R_6	10 M		
R_7	910 k		
R_8	110 k		
R_9	2.2 M		
R_{10}	820 k		
R_{11}	220		
R_{12}	10 M		
R_{13}	11 M		
R_{14}	820 k		

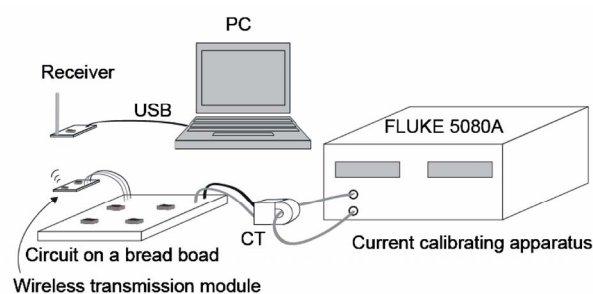
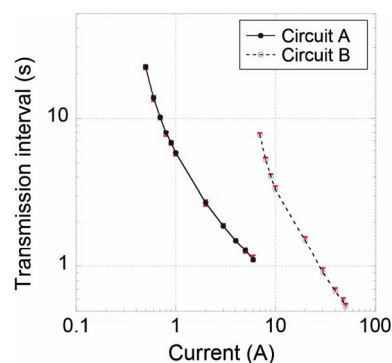
The voltage V_5 needs to exceed V_{T4} at I_{th_down} . In the circuit B, the wireless transmissions were sometimes not performed if V_{T4} equaled to V_{T1} . The reason has not clarified but we thought ripples generated by the step up converter can affect the stability. Thus, we determined V_{T4} was 2.26 V. If the resistance values of $R_{12,13}$ were set to 10 M Ω and 11 M Ω , respectively, it was found that V_5 exceeded V_{T4} at 220 Ω of the resistance R_{11} . The resistance values of $R_{5,6}$ were set to change the output of U_2 from low to high level at I_{th_down} . In this case, V_{T3} was 3.61 V.

Figure 5 shows the experimental setup. In this measurement, current calibrating apparatus (FLUKE 5080 A), the maximum current of which is 20.5 A, was used. When we measured transmission interval at more than 20.5 A, the power line was wrapped one time or two times and clamped the double or triple power lines. The frequency of AC current was 50 Hz. The transmission interval was measured by a receiver system that can save times when the receiver receives packets.

Figure 6 shows the results. The solid and dotted line indicates that the transmissions were performed using the power charged by the circuit A and circuit B, respectively. The each point is the average of ten measured intervals and the error bars are also shown. This graph shows this wireless sensor node can measure current from 0.5 A to 50 A. **Table 2** shows the differences between this work and [5].

4. Conclusion

In this research, the battery-less wireless current sensor

**Figure 5. Experimental setup.****Figure 6. Relationship between current flowing through a power line and transmission interval.****Table 2. Differences between this work and [5].**

	This work	[5]
Number of CTs	1	1
Number of charging circuits	2	1
Example of measurable range	0.5 A - 50 A (Double digits)	2 A - 20 A (Single digit)

node using that the charging time is depend on the current flowing through a power line was developed. In this type of sensor, there is a problem that the measurable range is about single digit since the charging time becomes short as the measured current increases. In this paper, we proposed the circuit in which two load resistors were used, and demonstrates that the node can measure current flowing through a power line from 0.5 A to 50 A. If the step-up converter and the resistors of $R_{1-6,12,13}$ are optimized or lower power consumed devices than the devices used in this research are utilized, the measurable range can be expanded.

REFERENCES

- [1] P. van de Ven, R. Feld, A. Bourke, J. Nelson and G. O. Laighin, "An Integrated Fall and Mobility Sensor and Wireless Health Signs Monitoring System," *Proceedings of IEEE Sensors*, Lecce, 26-29 October 2008, pp. 625-628.

- [2] S. G. Taylor, K. M. Farinholt, E. B. Flynn, E. Figueiredo, D. L. Mascarenas, E. A. Moro, G. Park, M. D. Todd and C. R. Farrar, "A Mobile-Agent-Based Wireless Sensing Network for Structural Monitoring Applications," *Measurement Science & Technology*, Vol. 20, No. 4, 2009, pp. 1-14. <http://dx.doi.org/10.1088/0957-0233/20/4/045201>
- [3] J. Hayes, S. Beirne, K.-T. Lau and D. Diamond, "Evaluation of a Low Cost Wireless Chemical Sensor Network for Environmental Monitoring," *Proceedings of IEEE Sensors*, Lecce, 26-29 October 2008, pp. 530-538.
- [4] T. Itoh, Y. Zhang, M. Matsumoto and T. Maeda, "Wireless Sensor Network for Power Consumption Reduction in Information and Communication Systems," *Proceedings of IEEE Sensors*, Christchurch, 25-28 October 2009, pp. 572-575.
- [5] H. Okada and T. Itoh, "Battery-Less Wireless Current Sensor Node Utilizing the Dependence of Charging Time of a Capacitor on the Current Flowing through a Power Line," *IEICE Electronics Express*, Vol. 10, No. 12, 2013. <http://dx.doi.org/10.1587/elex.10.20130308>
- [6] J. D. Cockcroft and E. T. S. Walton, "Experiments with High Velocity Positive Ions. (I) Further Developments in the Method of Obtaining High Velocity Positive Ions," *Proceedings of the Royal Society A*, Vol. 136, 1932, pp. 619-630. <http://dx.doi.org/10.1098/rspa.1932.0107>
- [7] Linear technology: datasheet of LTC1540, p. 5.
- [8] Silicon laboratories: datasheets of C8051F93x-C8051F92x, p. 46.
- [9] Nordic semiconductor: datasheets of nRF24L01, p. 13.